Cyclic behaviour and fatigue of stainless steels

M. Chauhan, J. Solin, J. Alhainen, T. Manninen, C. Lönnqvist

The cyclic stress-strain curve is used for describing a stabilized (averaged) stress-strain response in strain concentrations. Importantly, it describes the extremes of the stabilized hysteresis loop. This data is needed for estimating fatigue life based on the strain-life method for components subjected to cyclic loading. A typical application for this calculation method is the design of exhaust manifolds and cylinder heads experiencing severe temperature cycles and thermal straining. Cyclic tests with variable and constant strain amplitude, as well as tensile tests have been carried out for three materials: 1.4307, 1.4404 and 1.4541 –type commercial stainless steels in order to study the material response. The formation of martensite was measured in the tests. Secondary hardening was observed with all strain amplitudes in 1.4307 and 1.4541 whereas in 1.4404, secondary hardening occurred only with the smallest test amplitude. Also, the fatigue life of 1.4404 tended to be shorter than that of 1.4307 and 1.4501 in the high cycle fatigue (HCF) regime.

Keywords:
Austenitic stainless steel, cyclic hardening, hysteresis loop, martensite, fatigue

INTRODUCTION

Industrial components may experience cyclic loading resulting from e.g. thermal transients. Even if the level of the loading is modest, there usually exist areas where the stresses and strains are locally high due to the geometry. These locations are called stress concentrations and are treated with care, when determining the service life of the component.

Strain-life methods are frequently utilized for assessing the fatigue life of such locations since it has been observed that at critical locations the response of the material is strain or deformation dependent [1]. The stresses and strains occurring at the critical location during typical load cycle need to be computed. The finite element method (FEM) provides a tool to handle difficult geometries, but in order to obtain realistic values of resulting stresses and strains, the material behaviour has to be described accurately. This can be done, by performing tests on the material and transferring the experimental data into computer model. However, the fatigue life prediction models such as Coffin-Manson model and S-N-curve related models assume that the material response in cyclic loading stabilizes after the initial stage. Since austenitic stainless steel do not stabilize, describing the material behaviour under cyclic loading becomes complicated and selecting proper fatigue parameters that describes the material state during whole life, becomes crucial to the reliability of the evaluation [2]. The matter of how to describe the cyclic behaviour of stainless steels has not been fully solved. The purpose of this paper is to describe the complex behaviour of austenitic stainless steels during cyclic loading and to identify different factors affecting the observed phenomena.

Michael Chauhan, Jussi Solin, Jouni Alhainen
VTT, Espoo, Finland

Timo Manninen
Outokumpu Stainless Oy, Tornio Research Centre, Finland

Christian Lönnqvist
Wärtsilä Finland Oy

Paper presented at the 7th European Stainless Steel Conference - Como, 21-23 September 2011, organized by AIM

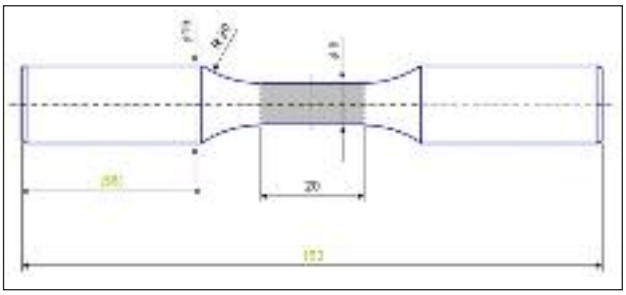

FIG. 1 ***Fatigue specimen and dimensions in mm.***
Provino utilizzato per le prove di fatica e sue dimensioni in mm.

Since largest strain amplitudes usually determine the material response (and thus the shape of the hysteresis loop), the magnitude of the applied amplitudes in the tests, should be set close to the ones that occur in practise [3]. Therefore, various tests were carried out with constant and variable strain amplitude. The variable amplitude tests were performed with a method called the spectrum-straining [4], in which the cyclic stress-strain curve (CSSC) is determined with a single specimen. The results of the constant and variable amplitude tests were compared. The cyclic response reveals the hardening/softening behaviour which correlates with the amount of accumulated plastic strain consequently affecting to the fatigue life.

EXPERIMENTAL

The three austenitic stainless steels were received as solution annealed 500mm×200mmx25mm plates. Samples were extracted from the sheet, turned and polished into smooth round bar specimens. Chemical compositions of the materials are given in Table 1 and the geometry and the dimensions of the fatigue bars are presented in Fig. 1

Tests were performed in a MTS 100kN rig with precision alignment

Material		wt %									
EN	ASTM	C	Si	Mn	P	S	Cr	Ni	Mo	N	Ti
1.4307	304L	0.02	0.3	1.7	0.03	0.001	18.2	8.1	-	0.07	-
1.4404	316L	0.02	0.5	1.4	0.03	0.001	17	10.2	2.5	0.04	-
1.4541	321	0.05	0.5	1.5	0.03	0.001	17.3	9.1	-	-	0.44

TAB. 1 ***Chemical composition of the test material.***

Composizione chimica dei materiali in prova.

	1.4307	1.4404	1.4541	
$Rp_{0.2}$	224	223	239*	Average of 2 tests
(MPa)	248	244	254	Material report
R_m	621	589	600*	Average of 2 tests
(MPa)	591	577	575	Material report

* Average of 3 tests

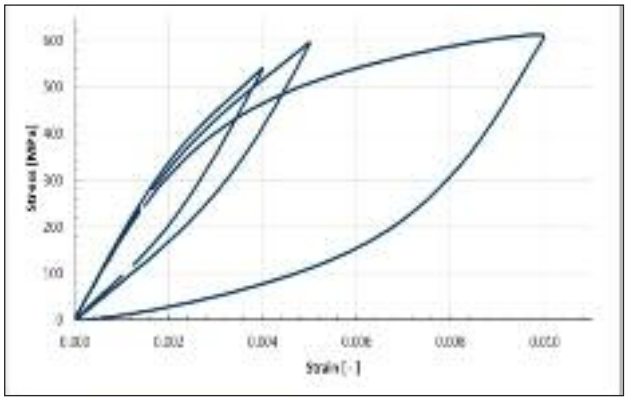

FIG. 2 ***Hysteresis loops of 1.4307 at half-life.***

Curva di isteresi dell'acciaio 1.4307 a metà vita.

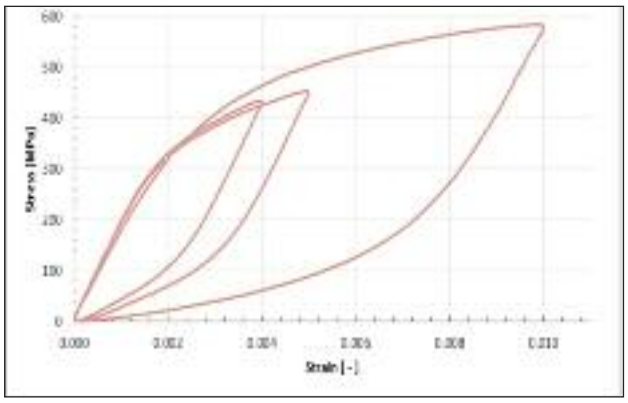

FIG. 3 ***Hysteresis loops of 1.4404 at half life.***

Curva di isteresi dell'acciaio 1.4404 a metà vita.

grips and digital control unit. Prior to actual tests, the alignment of load train was adjusted according to ASTM E 1012-05 procedure, using specimen with strain gauges. The strains were measured using MTS extensometers with gage lengths of 50 mm for tensile test and 8 mm for fatigue tests.

For each material, a tensile test was performed with pulling rate varying from 0,1 mm/min to 0,2 mm/min up till five percentages strain an after that with 0,5 mm/min. Partial unloadings were performed during the tensile test in order to measure the change in the elastic modulus as a function of strain. The strength properties of the test material are presented in Table 2.

TAB. 2
Monotonic strength properties.

Proprietà monotoniche di resistenza meccanica.

Strain, ε [-]	Number of cycles per block
0.025	8
0.05	8
0.075	8
0.1	8
0.125	8
0.15	8
0.175	8
0.2	8
0.225	8
0.25	10
0.3	7
0.35	5
0.4	3
0.45	2
0.5	1
	Σ100

TAB. 3
Test matrix for spectrum straining.

Matrice di prova per lo spettro delle deformazioni.

Strain controlled fatigue tests were carried out according to the ASTM E 606 procedure, using sinusoidal waveform. The constant amplitude tests were performed with a constant frequency, the average strain rate being 0,02 s^{-1} (e.g. 1Hz for ε_a) and the spectrum straining with the average rate of 0,01 s^{-1}. During the spectrum straining, the frequency was varied in order to maintain constant average strain rate, but the waveform was sinusoidal also in these tests.

The spectrum-straining was carried out by creating an arbitrary cyclic strain spectrum, consisting of 100 cycles, (maximum amplitude being ±0,5%), that was repeated until 25% load drop occurs for the largest cycle. This way, the CSSC can be determined with a single specimen. The test matrix for the spectrum straining is presented in Table 3.

RESULTS AND DISCUSSION

CONSTANT STRAIN AMPLITUDE TESTS

During constant strain amplitude tests, the stress amplitude and mean stress fluctuate, revealing the material response. The cyclic behaviour was studied through hysteresis loops and hardening/softening curves. Hysteresis loops at half-life ($N=N_{25}/2$, where N_{25} is the cycle number when 25% load drop occurs) for materials 1.4307, 1.4404 and 1.4541 loaded with strain amplitudes 0,2%, 0,25% and 0,5% are presented in Fig. 2-Fig. 4 respectively. The loops are positioned so, that every loop has the same minimum point.

The stress response at 0,25% strain amplitude was somewhat smaller than that at 0,2% amplitude for 1.4541. It must be noted however, that the amount of cycles at half-life for 0,2% was $2 \cdot 10^6$ whereas that for 0,25% was $1 \cdot 10^5$. It follows that the secondary hardening has advanced further in the specimen loaded with smaller am-

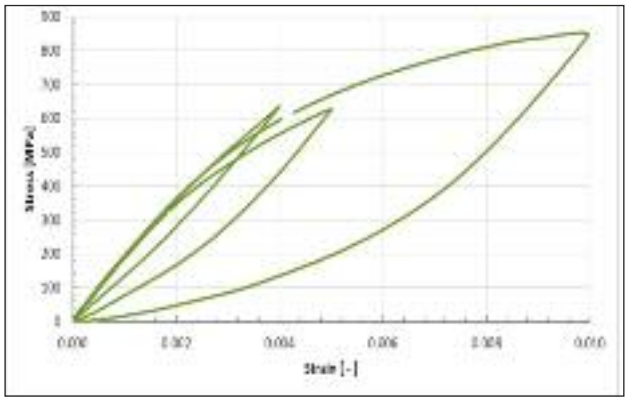

FIG. 4 ***Hysteresis loops of 1.4541 at half-life.***
Curva di isteresi dell'acciaio 1.4541 a metà vita.

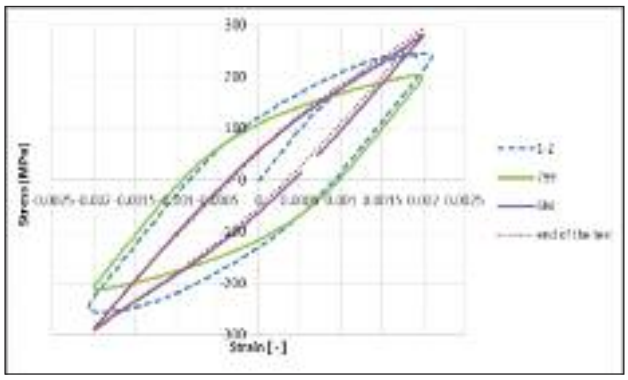

FIG. 5 ***Evolution of the hysteresis loop of 1.4307 (test interrupted at N=7912000).***
Evoluzione delle curve di isteresi dell'acciaio 1.4307 (prova interrotta a N=7912000).

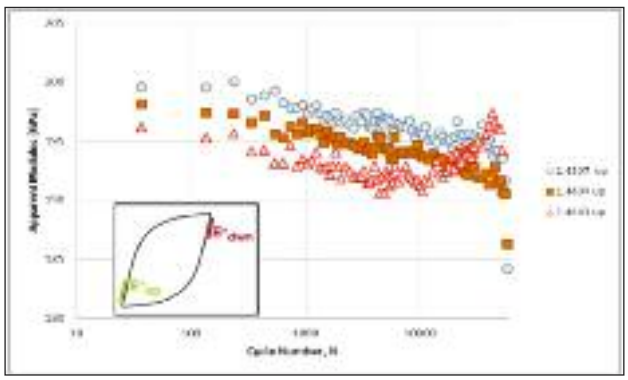

FIG. 6 ***Change of modulus in increasing ramps of hysteresis loops during cyclic straining.***
Cambiamento nel modulo col susseguirsi delle rampe delle curve di isteresi durante la deformazione ciclica.

plitude.
Comparison of the hysteresis loops with different amplitude reveals different strain hardening paths i.e. non-Masing behaviour. This implies that the dislocation microstructure is amplitude dependent. However, the deformation mechanism seems to change even during a single test, which can be seen as changes in the shape of the hysteresis loop in Fig. 5. At the beginning of the test, the proportion of plastic strains is notably higher than in the end. This is believed to reflect evolution of the microstructure.

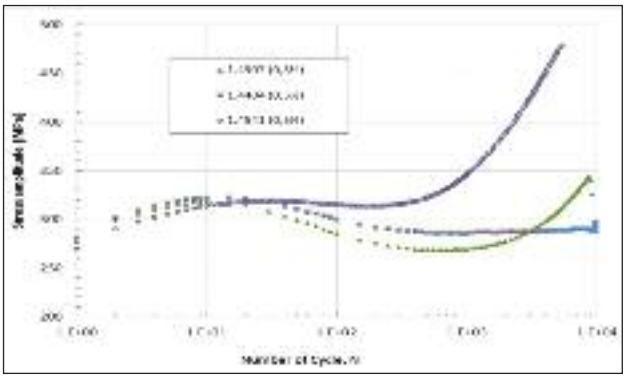

FIG. 7 ***Cyclic softening/hardening at 0,5% strain amplitude.***
Raddolcimento/incrudimento ciclico allo 0,5% di ampiezza di deformazione.

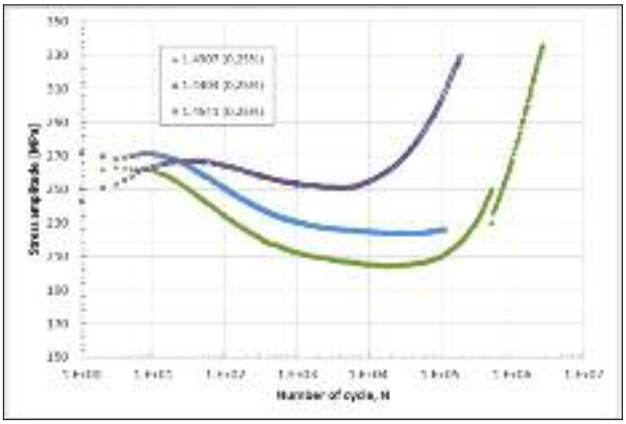

FIG. 8 ***Cyclic softening/hardening at 0,25% amplitude.***
Raddolcimento/incrudimento ciclico allo 0,25% di ampiezza di deformazione.

Fluctuation in the slope of the linear part of the hysteresis loop (modulus) is also believed to be induced partly by the internal (back) stresses. Systematic drop of modulus was observed at all strain amplitude levels and during the whole fatigue life for 1.4307 and 1.4404 whereas for 1.4541 upturn took place after initial descent. Evolution of modulus at maximum amplitude (0,5%) during spectrum straining is presented in Fig. 6

CYCLIC SOFTENING AND HARDENING

Softening/hardening curves are ideal for presenting the cyclic response during constant strain amplitude tests. They show the stress amplitude ($S_a = \Delta S/2$) as a function of number of cycles. The stress amplitudes of all three materials versus number of cycles during constant amplitude (0,5% and 0,25%) tests are presented in Fig. 7 and Fig. 8.
The cyclic stress responses proved to be consistent and well repeatable. Three evident phases were observed in 1.4541 and 1.4307 with all strain amplitudes: hardening, softening and secondary hardening, whereas in 1.4404, the secondary hardening occurred only at 0,19% strain amplitude (Fig. 9). During the initial hardening, dislocation density and internal stresses are increased. Repeated loading enhances the re-organization of dislocation structure, which is observed as cyclic softening. Most of the fatigue life is spent during secondary hardening, during which the amount of plastic strains per cycle decreases as stress amplitude increases.

CYCLIC STRESS-STRAIN CURVES

The cyclic stress-strain data can also be presented as cyclic stress-

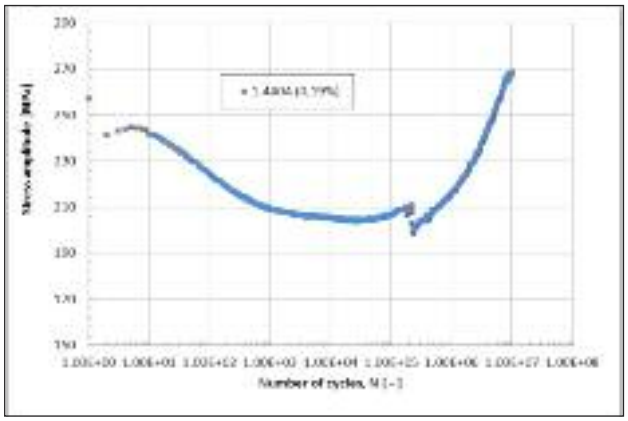

FIG. 9 ***Cyclic softening/hardening of 1.4404 at 0,19% amplitude***

Raddolcimento/incrudimento ciclico dell'acciaio 1.4404 allo 0,10% di ampiezza di deformazione.

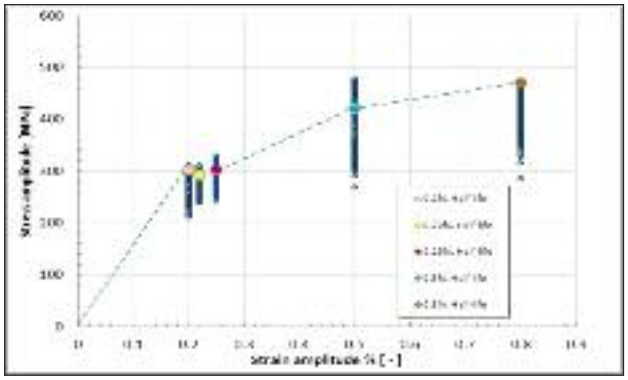

FIG. 10 ***Constant amplitude data of 1.4541 in CSSC format. The small dots present the variation in the stress amplitude.***

Dati dell'ampiezza costante dell'acciaio 1.4541 nella rappresentazione CSSC (cyclic stress-strain curves). I piccoli punti mostrano la variazione dell'ampiezza di carico.

strain curves (CSSC) in which the stress amplitude is plotted against strain amplitude. The cyclic stress-strain curve (CSSC) is traditionally presented as the half-life response of the material during constant amplitude (or ramp loading). However, this is badly suited for stainless steels which do not stabilize in cyclic deformation. For austenitic stainless steels, the spectrum-straining method is more applicable [5]. Stress responses during different constant strain amplitude tests in CSSC coordinates are presented in Fig. 10. Also the fluctuation in the stress amplitude during whole test is shown. Secondary hardening is pronounced at strain amplitudes 0,5% and 0,8%.

An alternative method for determining CSSC is spectrum straining. CSSCs determined at different phases of the test and Ramberg-Osgood fittings are presented for all three materials in Fig. 11-13 and the determined Ramber-Osgood parameters in Table 4. It can be seen that 1.4307 and 1.4404 behave quite similarly; the stress response at half-life being quite the same as in the end, even though in 1.4307 a minor increase in the stress amplitude is observed. However, 1.4541 continues to harden till the end. The half-life responses during constant amplitude and spectrum straining tests are compared in Fig. 14.

HARDENING BEHAVIOUR

Strain hardening, which is observed in all three materials, is a com-

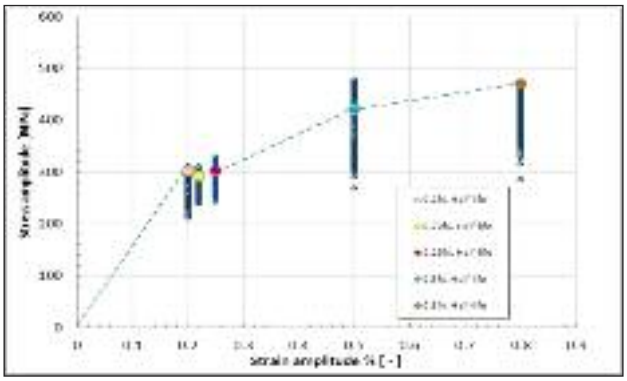

FIG. 11 ***CSSC and Ramberg-Osgood fitting of 1.4307. Ramberg-Osgood fitting marked as R-O.***

Rappresentazioni secondo CSSC e Ramberg-Osgood per l'acciaio 1.4307. Le risultanze del modello Ramberg-Osgood sono contrassegnate come R-O.

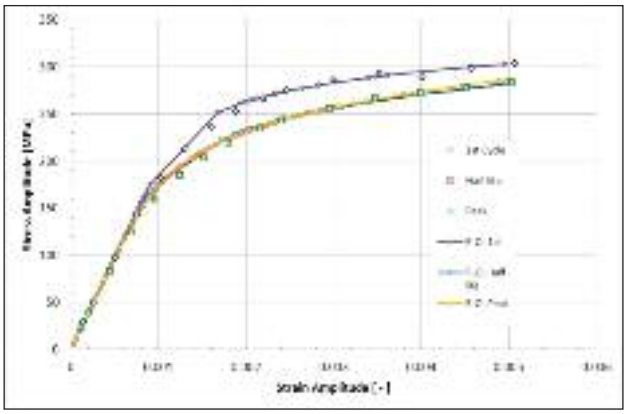

FIG. 12 ***CSSC and Ramberg-Osgood fitting of 1.4404. Ramberg-Osgood fitting marked as R-O.***

Rappresentazioni secondo CSSC e Ramberg-Osgood per l'acciaio 1.4404. Le risultanze del modello Ramberg-Osgood sono contrassegnate come R-O.

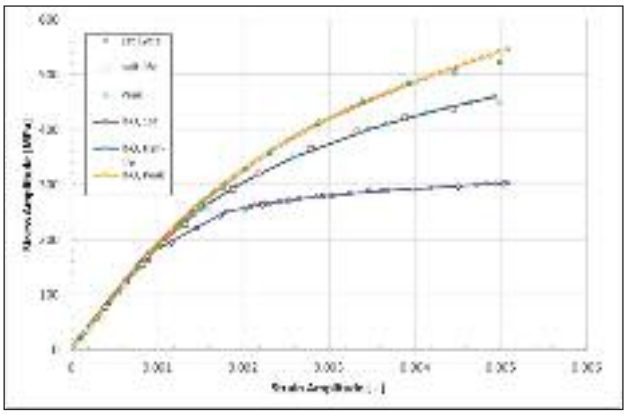

FIG. 13 ***CSSC and Ramberg-Osgood fitting of 1.4541. Ramberg-Osgood fitting marked as R-O.***

Rappresentazioni secondo CSSC e Ramberg-Osgood per l'acciaio 1.4307. Le risultanze del modello Ramberg-Osgood sono contrassegnate come R-O.

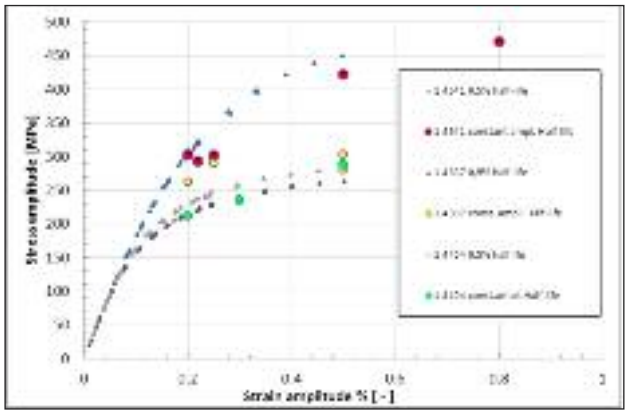

FIG. 14 ***Summary of CSSCs.***

Sommario dei risultati del modello CSSC.

mon phenomenon for cold worked stainless steel. As the material is repeatedly loaded, amount of dislocations and mechanical twins increase. These work as glide obstacles for other dislocations.

Strain hardening may also occur due to strain-induced martensite formation. The face-centered cubic microstructure of most austenitic stainless steels is not thermodynamically stable at room temperature. Therefore, applied loading may induce a diffusionless martensitic phase transformation. The stability of austenite against strain-induced martensitic transformation depends on the chemical composition and microstructure of the austenite. Low austenite stability results in a pronounced tendency to martensite formation. Therefore, the stability of austenite determined the mechanism of strain hardening.

At present, it is believed, that the strain induced martensite formation may occur via to two different transformation paths: $\gamma \rightarrow \varepsilon \rightarrow \alpha'$, or directly $\gamma \rightarrow \alpha'$.

The formation of α'-martensite is related to shear bands, which are deformation structures consisting of stacking fault bundles, ε-martensite, deformation twins, or some mixture of these. The strain induced α'-martensite is believed preferably to nucleate at shear bands, especially at intersections of shear bands and since the amount of shear bands increases with deformation, it consequently increases the amount of α'-martensite nucleation locations. Many investigations have shown that the ε-martensite phase precedes the formation of α'-martensite and that the volume fraction of ε-martensite decreases after reaching a certain maximum while α'-martensite volume fraction increases with deformation. It follows that the transformation route would be $\gamma \rightarrow \varepsilon \rightarrow \alpha'$ [6,7,8]. However, Das et al. [9] observed α'-martensite formation in a single shear band and grain boundary triple points. It was concluded that both transformation routes are possible even for the same stainless steel.

In order to study the hardening behaviour, the amount of ferrite was measured from the test specimens. The measurements were performed using Fisher Ferritoscope MP30, which determines the magnetic permeability of the material. The results presented in Fig. 15 are averaged over four measurements. The measured amount of ferrite must be multiplied by the factor 1,7 in order to determine the amount of martensite in the material [10].

Hong et al. [2] concluded that the cumulative plastic strain (which adds defects to the material) must exceed a critical value for the plasticity-induced martensite transformation to occur. The results of the ferrite contents measurement and hardening/softening curves (Fig. 7-9 and Fig. 15) reveal that the critical value differs from one material to other as the initiation of secondary hardening varies between materials. Due to the earlier initiation, the volume fraction of martensite tends to be larger in 1.4541 than in 1.4307. The ferrite contents of 1.4307 is higher than 1.4541 only in the specimen loaded with strain amplitude of 0,25%. This is due to the significantly longer fatigue life of 1.4307, which results in higher amount of accumulated plastic strain.

The clear correlation between cyclic response and ferrite contents can also be seen from the CSSCs (Fig. 11-13) and ferrite content measurements. Cyclic response of 1.4307 at half-life and at end is similar to that of 1.4404 and also the ferrite contents are almost equal. It is interesting, that even though microstructure of the material is thought to be governed by the largest strain amplitude, apparently, the amount of large cycles in variable amplitude loading is not sufficient to initiate the secondary hardening in 1.4307, even though the phenomenon is clear during constant amplitude loading. This implies that in order to determine the cyclic response of the stainless steel for practical application under variable amplitude loading, the magnitude of the largest amplitude as well as their number in the test spectrum should be chosen as close as possible to the operational loading in practise. On the other hand, it has been reported [2], that by using the plastic strain energy as a fatigue parameter, the complications related to the non-stabilization of stainless steel may be avoided. Plastic strain energy is a combination of stress and plastic strain, which are inversely related. Thus positive change in other is compensated as negative change in the other.

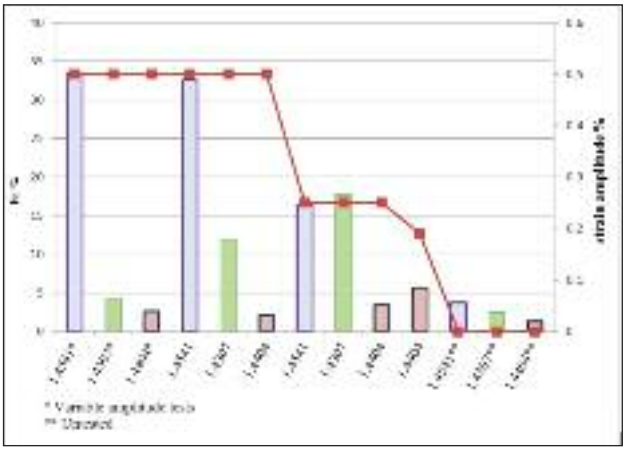

FIG. 15 ***Measured ferrite contents. The red line presents the strain amplitude and in the case of variable amplitude test, it presents the maximum amplitude.***

Contenuti di ferrite misurati. La linea rossa mostra l'ampiezza della deformazione e, nel caso della prova ad ampiezza variabile, riporta l'ampiezza massima.

TAB. 4
Determined Ramberg-Osgood parameters.

Parametri del modello Ramberg-Osgood determinati.

	1.4307		1.4404		1.4541	
	n'	K'	n'	K'	n'	K'
1st	0.077	447.6	0.0857	493.25	0.0981	527.12
Half-life	0.1502	619.61	0.1305	588.71	0.2344	1857.3
Peak	0.1711	727.55	0.1473	657.89	0.2683	2778.1

FATIGUE LIFE

The results of the constant strain amplitude fatigue tests are presented in Fig. 16. Purely based on the tests performed within this study, it can be concluded, that the fatigue strength of 1.4404 is good in the LCF regime, whereas the fatigue strengths of 1.4307 and 1.4541 are better in the HCF regime. Secondary hardening and slightly increased ferrite contents in 1.4404 were observed only in the specimen loaded with 0,19% stain amplitude. The test resulted as a run-out after 10 million cycles, but as can be seen from the fatigue test results, 1.4404 loaded with 0,2% strain amplitude resulted in much shorter fatigue life.

The fatigue life of 1.4404 is much shorter at strain amplitudes 0,2% and 0,25% than that of 1.4307 or 1.4541. This may origin from the fact that secondary hardening does not occur in the more stabile 1.4404 and so the amount of accumulated plastic strain is greater than it is in 1.4307 or 1.4541, where significant secondary hardening and increased ferrite contents were observed. Conversely, in the low cycle fatigue (LCF) regime, where significant ferrite contents were also measured in 1.4541, 1.4307 and 1.4404 lasted longer. The positive effect of decreasing the amount of plastic strain is commonly acknowledged. Nikitin [11] for instance, observed during load controlled tests, that high test frequency resulted in increased temperature in the specimen. The higher temperature inhibits the martensitic transformation which further decreased the fatigue life compared to the specimen loaded with lower frequencies. However Muller-Bollenhagen et al. [12] adjusted the martensite volume fraction of AISI304 test specimen by a tensile load prior to load-increase fatigue tests, In their experiments, the fatigue strength initially increased with martensite content, the optimal being 19%, but larger initial volume fractions than that, were found to have a negative influence to the fatigue life.

CONCLUSIONS

The measurements of cyclic stress-strain response of 1.4307, 1.4404 and 1.4541 resulted in the following conclusions:

- The spectrum straining method was found suitable for determining the cyclic stress-strain curve (CSSC) for these materials and the curve can be expressed with the Ramberg-Osgood equation.
- The constant amplitude tests showed initial hardening, followed by a softening phase in all three materials. There was secondary hardening in 1.4307 and 1.4541, with all strain amplitudes. In 1.4404 secondary hardening did not occur with stain amplitudes above 0,19%.
- After the spectrum straining and constant amplitude tests an increased ferrite content was measured from 1.4541. The measured ferrite content of 1.4307 was lower than in 1.4541, except in the tests performed with 0,25% strain amplitude, where the fatigue life of 1.4307 was significantly longer. In 1.4404 the ferrite content changes were relatively small.

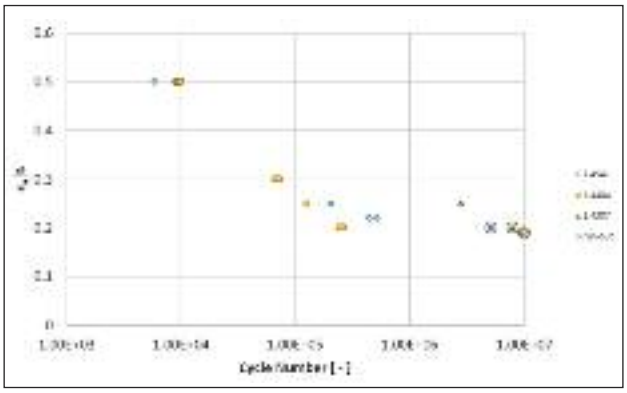

FIG. 16 ***Fatigue test results.***

Risultati delle prove di fatica.

- The cyclic response does not stabilize, but the magnitude and for the case of variable amplitude loading the number of occurrences of the largest cycles determines the cyclic response of 1.4541, 1.4404 and 1.4307.

ACKNOWLEDGEMENTS

The work has been done within FIMECC Ltd and its DEMAPP program. We gratefully acknowledge the financial support from Tekes and the participating companies.

REFERENCES

1. J. BANNANTINE, J. COMER, J. HANDROCK. Fundamentals of Metal Fatigue Analysis. Prentice Hall, New Jersey (1987), p.39.
2. S.G. HONG, S.B. LEE, T.S. BYUN, Mater. Sci. Eng. A 457 (2007), p.139.
3. J. SOLIN, G. NAGEL and W. MAYINGER, Proc. PVP 2009-78138 2009 ASME Pressure Vessel and Piping Division Conference, Prague, Czech Republic (2009).
4. J. SOLIN. Fatig Eng Mat Struct, IMechE (C245/86) vol. 1, (1986) , p. 273
5. J. SOLIN. VTT Research reports 647, VTT, Technical Research Centre of Finland, Espoo (1989), p.42
6. A. OIKARI, Deformation Mechanisms and Strain Hardening of Chromium-Manganese-Nickel Alloyed Austenitic Stainless Steels. Master's thesis. Aalto University School of Science and Technology. (2010), p.49.
7. K.H. LO, C.H. SHEK and J.K.L. LAI, Mater. Sci. Eng. R65 (2009), p.39.
8. G. BAUDRY, A. PINEAU, Mater. Sci. Eng. A 28 (1977), p.229.
9. A. DAS, S. SIVAPRASAD, M. GHOSH, P.C. CHAKRABORTI and S. TARAFDER, Mater Sci Eng A 486 (2008), p. 283.
10. J. TALONEN, P. ASPEGREN and H. HÄNNINEN, Mater. Sci. Technol. 12 (2004), p.1506.
11. I NIKITIN, M. BESEL, Int J Fatigue 30 (2008), p.2044.
12. C. MULLER-BOLLENHAGEN, M. ZIMMERMANN and H.-J. CHRIST, Int. J. Fatigue 32 (2010), p. 936.

Abstract

Comportamento ciclico e a fatica di acciai inossidabili

Parole chiave: acciaio inossidabile - fatica

La curva ciclica carico-deformazione viene utilizzata per descrivere la risposta tensione-deformazione stabilizzata (media) nelle concentrazioni delle deformazioni. È molto importante per descrivere gli estremi del ciclo di isteresi stabilizzato. Questi dati sono necessari per stimare la vita a fatica sulla base del metodo vita-deformazione per componenti soggetti a carichi ciclici. Una tipica applicazione di questo metodo di calcolo è la progettazione di guarnizioni di testata e di collettori di scarico che sono sottoposti a severi cicli di temperatura e deformazioni termiche. Per studiare la risposta dei materiali sono state effettuate prove cicliche con ampiezza di deformazione sia variabile che costante, oltre a prove di trazione, su tre diversi acciai inossidabili commerciali, quali 1.4307, 1.4404 e 1.4541. La formazione della martensite è stata misurata nell'ambito delle prove. Per tutte le ampiezze di deformazione è stato osservato un incrudimento secondario negli acciai 1.4307 e 1.4541, mentre per l'acciaio 1.4404 l' incrudimento secondario si è verificato solo con l'ampiezza di prova più bassa. Inoltre, la vita a fatica dell'acciaio 1.4404 ha mostrato una tendenza ad essere inferiore rispetto a quella degli acciai 1.4307 e 1.4501 in regime di cicli di fatica elevati (HCF).